Deep-Sea Research I 85 (2014) 47–55

Contents lists available at ScienceDirect

Deep-Sea Research I

journal homepage: www.elsevier.com/locate/dsri

A role for nitrite in the production of nitrous oxide in the lower euphotic zone of the oligotrophic North Pacific Ocean

Samuel T. Wilson [a,b,*], Daniela A. del Valle [a,b], Mariona Segura-Noguera [a,b], David M. Karl [a,b]

[a] Department of Oceanography, School of Ocean and Earth Science and Technology, University of Hawaii, Honolulu, HI 96822, United States
[b] Center for Microbial Oceanography: Research and Education, University of Hawaii, 1950 East-West Road, Honolulu, HI 96822, United States

ARTICLE INFO

Article history:
Received 23 July 2013
Received in revised form
19 November 2013
Accepted 29 November 2013
Available online 13 December 2013

Keywords:
Nitrous oxide
Nitrite
Ammonium
Nitrifier-denitrification
Oligotrophic
Euphotic-zone

ABSTRACT

Understanding the role of the oceans in the Earth's changing climate requires comprehension of the relevant metabolic pathways which produce climatically important trace gases. The global ocean represents one of the largest natural sources of nitrous oxide (N_2O) that is produced by selected archaea and/or bacteria during nitrogen (N) metabolism. In this study, the role of nitrite (NO_2^-) in the production of N_2O in the upper water column of the oligotrophic North Pacific Subtropical Gyre was investigated, focusing primarily on the lower euphotic zone where NO_2^- concentrations at the primary NO_2^- maximum reached 195 nmol L^{-1}. Free-drifting sediment trap arrays were deployed to measure N cycle processes in sinking particulate material and the addition of selected N substrates to unpreserved sediment traps provided an experimental framework to test hypotheses regarding N_2O production pathways and controls. Sinking particles collected using NO_2^--amended, unpreserved sediment traps exhibited significant production of N_2O at depths between 100 and 200 m. Subsequent stable isotope tracer measurements conducted on sediment trap material amended with $^{15}NO_2^-$ yielded elevated $\delta^{15}N$ values of N_2O, supporting N_2O production via a NO_2^- metabolism pathway. Experiments on seawater collected from 150 m showed N_2O production via NO_2^- metabolism also occurs in the water-column and indicated that the concentration of NO_2^- relative to NH_4^+ availability may be an important control. These findings provide evidence for the production of N_2O via nitrifer-denitrification in the lower euphotic zone of the open ocean, whereby NO_2^- is reduced to N_2O by ammonia-oxidizing microorganisms.

© 2013 Elsevier Ltd. All rights reserved.

1. Introduction

Nitrous oxide (N_2O) is a potent greenhouse gas influencing Earth's climate by absorbing infrared radiation and acting as a precursor to stratospheric ozone depleting radicals (Ravishankara et al., 2009). In the open ocean, concentrations of dissolved N_2O in the upper 100 m of the water column typically range from 7 to 9 nmol L^{-1} and are therefore typically slightly supersaturated (104–130%) with respect to atmospheric equilibrium (*e.g.* Dore and Karl, 1996a; Forster et al., 2009; Bange et al., 2010). This results in an ocean-atmosphere flux of N_2O that has been estimated to contribute approximately 20% of the total N_2O in the atmosphere (Denman et al., 2007).

N_2O is produced as a by-product of nitrogen (N) metabolism and inoxygenated seawater is typically ascribed to nitrification whereby ammonia (NH_3) is oxidized via hydroxylamine to nitrite (NO_2^-) (Fig. 1). The strong correlation between N_2O and apparent oxygen utilization (AOU) is considered supporting evidence for N_2O production derived from nitrification (Dore et al., 1998; Nevison et al., 2003). In recent years, our understanding of N_2O in the ocean has improved with the application of molecular (*e.g.* Rotthauwe et al., 1997; Mincer et al., 2007) and stable isotope (*e.g.* Ostrom et al., 2000; Sutka et al., 2006; Santoro et al., 2011) technologies to identify the microorganisms and metabolic pathways responsible for N_2O production. A major discovery was that archaea significantly contribute to the production of N_2O production in the marine environment (Francis et al., 2005; Santoro et al., 2010, 2011; Löscher et al., 2012).

However the specific details underlying N_2O production via nitrification in the open ocean remain unclear. In this study, the role of NO_2^- in the production of N_2O at the base of the euphotic zone is investigated. NO_2^- is not an immediately obvious candidate for stimulating N_2O production in aerobic habitats. The redox state of NO_2^- limits its direct involvement in N_2O cycling in the upper ocean as oxidation to NO_3^- is not known to yield N_2O and denitrification is not considered significant in well-oxygenated seawater, except possibly in the interior of large particles (Karl et al., 1984). Furthermore, NO_2^- concentrations are generally low (< 20 nmol L^{-1}) in the open ocean, with the exception of the distinct peak at the base of the euphotic zone referred to as the primary NO_2^- maximum (PNM) (Lomas and Lipschultz, 2006). It

* Corresponding author at: Department of Oceanography, School of Ocean and Earth Science and Technology, University of Hawaii, Honolulu, HI 96822, United States. Tel.: +1 808 956 0573.
E-mail address: stwilson@hawaii.edu (S.T. Wilson).

0967-0637/$ - see front matter © 2013 Elsevier Ltd. All rights reserved.
http://dx.doi.org/10.1016/j.dsr.2013.11.008

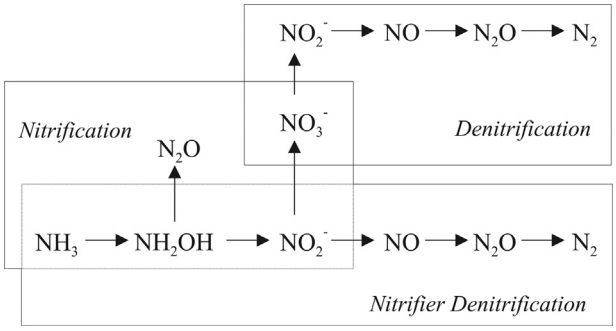

Fig. 1. Schematic diagram of the nitrification, denitrification, and nitrifier-denitrification pathways (redrawn from Wrage et al., 2001). The production of N_2O (and also NO and N_2) via nitrifier-denitrification is not well understood at present.

has been proposed that the PNM results from ammonia-oxidizing microorganisms that oxidize NH_3 to NO_2^- (Olson, 1981). However other studies indicate that the PNM most likely reflects an imbalance in phytoplankton N exudation, due to incomplete assimilation of NO_3^- (Kiefer et al., 1976; Lomas and Lipschultz, 2006). In the North Pacific Subtropical Gyre (NPSG), both processes appear to contribute to the PNM although there may be a subtle vertical segregation leading to distinct upper and lower PNM processes (Dore and Karl, 1996b).

Nonetheless there are several lines of evidence that NO_2^- plays an active role in the production of N_2O. The release of N_2O via NO_2^- metabolism is currently referred to as the 'nitrifier-denitrification' pathway whereby NO_2^- is reduced to NO and then to N_2O analogous to the classic denitrification pathway (Fig. 1). The nitrifier-denitrification pathway has been identified in laboratory-maintained cultures of ammonia-oxidizing bacteria (Shaw et al., 2006; Frame and Casciotti, 2010) and ammonia-oxidizing archaea (Santoro et al., 2011).

In this study, we evaluate N cycling in the surface ocean from a series of water column measurements, on-deck incubations, and amendment experiments conducted using free-drifting sediment trap arrays in the oligotrophic North Pacific Subtropical Gyre. Our findings indicate that NO_2^- metabolism represents a possible microbial metabolic pathway for N_2O production in both sedimenting particles and those suspended in the water column. We discuss how nitrifier-denitrification can be accommodated into our current understanding of N_2O dynamics and the wider N cycle in the marine environment.

2. Methods

2.1. Oceanographic fieldwork

The fieldwork was conducted onboard the R/V *Kilo Moana* during three oceanographic cruises in the NPSG. The water column profiles and sediment trap experiments were conducted at 24° 45′N, 157° 45′W, approximately 100 nautical miles to the north of Station (Stn) ALOHA (Karl and Lukas, 1996) in September 2011 during the BioLINCS cruise. Additional experiments were conducted at Stn ALOHA (22° 45′N, 158°W) in February and June 2013 during HOT cruise 249 and 253, respectively.

2.2. Hydrographic and biogeochemical measurements

The hydrographic conditions of the water column were measured using a conductivity, temperature, and depth (CTD) rosette system coupled with chlorophyll fluorescence (Seapoint) and O_2 (SeaBird SBE 43) sensors. The fluorescence and O_2 sensors were calibrated using discrete fluorometric analysis of chlorophyll *a* (Strickland and Parsons, 1972) and dissolved O_2 (Carritt and Carpenter, 1966), respectively. The water column was sampled for a range of biogeochemical parameters using Niskin-like 'Bullister' bottles attached to the CTD-rosette. Of specific interest to this study are the measurements of nitrogenous nutrients, particulate carbon/nitrogen (POC/PON), and N_2O. Seawater samples for nutrient analysis (NH_4^+, NO_2^-, and NO_3^-) were collected into acid-washed 125 mL polyethylene bottles, capped, and then stored frozen. NO_2^- and NH_4^+ concentrations were quantified onboard with the spectrophotometer method described in Hansen and Koroleff (1999) using a liquid core waveguide with a 2 m pathlength for added sensitivity. Nutrient analysis for NO_2^- plus NO_3^- was performed on land using a Bran+Luebbe Autoanalyzer III when NO_3^- concentrations exceeded 0.1 μmol L^{-1} (*i.e.* for samples collected below a depth of 100 m) and using a chemiluminescence technique with its greater detection limit of 1 nmol L^{-1} for the upper water-column (0–100 m) samples (Dore and Karl, 1996b). NO_3^- concentrations were subsequently calculated from both sets of analyses by subtracting NO_2^- values. Seawater samples for PON were collected onto 25 mm diameter combusted (450 °C, 5 h) and acid-washed glass fiber filters (Whatman GF/F). The filters were stored frozen until analysis using a Carlo Erba NC 2500 elemental analyzer with a Finnigan MAT ConFlo II coupler with acetanilide (C_8H_9NO) and dried plankton material used as the primary and secondary standards, respectively.

Seawater samples for N_2O analysis were collected in either 76 or 240 mL crimp sealed vials. Sample bottles were filled from the bottom to at least three times overflowing, and poisoned with 200 μL of saturated mercuric chloride ($HgCl_2$) solution. N_2O concentrations were determined using a gas chromatograph (GC) (Agilent 7890A) fitted with an electron capture detector (ECD). A weighed sub-sample was transferred from the sample bottle to a 250 mL purge chamber under positive pressure and sparged using helium at 80 mL min^{-1}. The gas stream subsequently passed through a nafion drier (Perma Pure LLC), drierite (VWR), and carbosorb (Europa Scientific) before being cold-trapped on a 1 mL sample loop containing PorapaK Q 80/100 (Sigma-Aldrich) submerged in a small dewar of liquid nitrogen. After purging, the sample loop was heated to 90 °C and injected onto a 30 m × 0.32 mm GS-CarbonPLOT capillary column (J&W Scientific) via a stainless steel 6-port switching valve (Valco). The GC oven temperature was 40 °C and the ECD was maintained at a temperature of 250 °C. The N_2 flow rate to the ECD was 60 ml min^{-1} and the carrier gas was helium at 1.6 mL min^{-1}. Data acquisition was performed using ChemStation software version B.03.01. The ECD was calibrated for N_2O using a 101 ppmv ($\pm$2%) primary standard in nitrogen (Scott-Marrin). Seawater concentrations were calculated with the functions for the Bunsen solubility coefficients provided by Weiss and Price (1980) with temperature and salinity provided by the CTD. Percent saturations were calculated using an atmospheric N_2O mixing ratio of 0.325 ppmv obtained from the Global Monitoring Division (GMD; http://www.esrl.noaa.gov/gmd/) of the National Oceanic and Atmospheric Administration/Earth System Research Laboratory (NOAA/ERSL).

For a separate set of experiments, seawater samples were amended with ^{15}N-labeled compounds and the relative $\delta^{15}N$ enrichment of N_2O was measured at the end of the incubation period. To determine the isotopic composition of N_2O, dissolved gases were purged from the seawater sample using a sparging set-up similar to that described above for quantifying concentrations. The gas sample was then cryofocused for a second time before injecting onto a Porobond Q (25 m × 0.32 mm) analytical column (J&W Scientific) maintained at 17 °C, using the method of Popp et al. (1995). N_2O was then introduced directly into the ion source of a MAT 252 isotope-ratio-monitoring gas chromatograph/mass spectrometer (irmGC/MS). N_2O concentration and stable-isotope ratios were measured simultaneously by monitoring the ion currents of masses 44, 45, and 46 using the Finnigan ISODAT

software. All isotopic values are reported as per mil deviations with respect to atmospheric N_2 using standard delta notation: $\delta^{15}N_{sample} = [(^{15}N/^{14}N_{sample}/^{15}N/^{14}N_{standard}) - 1] \times 1000$. The reference standard is atmospheric N_2 gas ($^{15}N/^{14}N = 0.0036765$, $\delta^{15}N = 0‰$). The calibration of N_2O concentration was achieved using a commercial gas mixture (100 ppmv), and double-checked using dilutions of high-purity N_2O in helium. All of the $^{15}N_2O$ measurements were conducted at the Stable Isotope Facility, University of Hawaii (www.soest.hawaii.edu/GG/isotope_biogeochem).

2.3. Field experiments: Sediment traps

Complementary to the water column profiles, experiments were conducted at sea to further investigate the relationship between NO_2^- and N_2O. We used sediment traps to characterize microbial activity associated with sinking particles and N amendments (both ^{15}N labeled and non-labeled) to help deduce N_2O production pathways and controls. The different treatments used in the sediment trap experiments are listed in Table 1. Some traps were deployed with preservative (formalin, final concentration of 1% by weight) to capture the flux and state of particles during their downwards trajectory and replicate traps were deployed without fixative to investigate the in situ activity of particle-associated microbes. In addition, two traps were amended with either ammonium chloride (NH_4Cl) or sodium nitrite ($NaNO_2$) (target final concentration of 100 μmol N L^{-1}) (Table 1) to test the predictions of our hypothesized nitrifier-denitrification pathway for N_2O production. All the sediment trap solutions were prepared 1 day before deployment and analyzed for the appropriate blanks and time zero samples.

The sediment trap array itself consisted of individual cylindrical traps attached to polyvinyl chloride (PVC) crosses at twelve predetermined depths of 100, 110, 120, 130, 140, 150, 160, 175, 200, 250, 300, and 500 m. The traps were identical in design to those used extensively in the VERTEX and HOT field programs (Knauer et al., 1979) with a cross-sectional area of 0.0039 m^2 and an aspect ratio of 7:1. The traps were fitted with a 335 μm Nitex screen at the base of the baffle to prevent large zooplankton from swimming into the solutions and potentially compromising the experiment (Karl and Knauer, 1989). Prior to deployment, all traps were filled with approximately 1.8 L of 0.2 μm filtered salt solution (Table 1) to prevent flushing of material from the traps during deployment/recovery and to retain all by-products of *in situ* microbial metabolism in the unpreserved traps including N_2O. The deployment and subsequent recovery of the trap lasted approximately 2 h and was conducted before dawn to avoid exposing the samples to sunlight. The trap array was deployed on September 9, 2011 at 24° 41.4′N, 157° 34.3′W and during 8 days it drifted approximately 20 nautical miles eastward, before being recovered at 24° 34.8′N, 157°01.3′W.

Table 1
Trap solutions and nutrient treatments for the sediment trap arrays deployed during September 2011 and February 2013. The salt solution was composed of sodium chloride (33.8 g L^{-1}), magnesium chloride (14.3 g L^{-1}), and potassium chloride (0.93 g L^{-1}) (Karl et al., 1984). Note that incubations in September 2011 were conducted *in situ*, and incubations conducted in February 2013 followed trap recovery.

Date	Treatment	Solution
Sept 2011	Preserved	Salts, Formalin
	Live (unamended)	Salts
	NH_4^+-amended	Salts, NH_4Cl (100 μmol L^{-1})
	NO_2^--amended	Salts, $NaNO_2$ (100 μmol L^{-1})
Feb 2013	Live (unamended)	Salts
	$^{15}NH_4^+$-amended	Salts, $^{15}NH_4Cl$ (4 μmol L^{-1})
	$^{15}NO_3^-$-amended	Salts, $Na^{15}NO_3$ (4 μmol L^{-1})
	$^{15}NO_2^-$-amended	Salts, $Na^{15}NO_2$ (4 μmol L^{-1})

After the free-drifting sediment trap array was recovered, the individual traps were sub-sampled to determine the relevant biogeochemical parameters. The same protocol was followed for each trap whereby the overlying seawater was removed and the sample was gently mixed using a custom-built stirring device designed to homogenize the trap contents, but prevent gas exchange with the atmosphere. The samples therefore reflect a combination of particles and their interstitial porewaters, the initial sediment trap solution, and by-products of microbial metabolism (for unpreserved traps). Dissolved gas samples for N_2O and O_2 were collected by carefully siphoning a portion of the homogenized trap samples into crimp-sealed borosilicate glass vials. Subsequently the traps were sampled for PON by filtering through a 25 mm combusted Whatman GF/F filter, and the filtrate collected for nutrient analysis. Samples for dissolved gases, PON, and nutrients were subsequently stored and analyzed in our shore laboratory as previously described for the water column measurements. The O_2 measurements were conducted by filling 12 mL Exetainer vials (Labco Ltd), preserving with $HgCl_2$ and analyzing the dissolved O_2 content using a membrane inlet mass spectrometer (MIMS). In brief, the MIMS provides rapid and accurate measurements of gas ratios by coupling semipermeable, Microbore tubing with the inlet vacuum line of a quadropole mass spectrometer (Kana et al., 1994). Reference measurements consisted of a 1 l reservoir of filtered (0.2 μm) surface seawater collected from Stn ALOHA. The analytical temperature for reference seawater and samples was kept constant at 23 °C by immersing the 1/16″ stainless steel inlet tubing inside a water bath. The gases analyzed included those with a mass of 32 and 40 (corresponding to O_2 and Ar) and in this study we report only the O_2 concentrations.

2.4. Field experiments: ^{15}N tracer studies

Additional trap experiments were conducted at Stn ALOHA during HOT cruise 249 (February 2013) to corroborate the findings from the September 2011 cruise. These experiments consisted of 12 individual unpreserved traps deployed at a single depth of 150 m for a 57 h period. This second set of sediment trap experiments employed the use of ^{15}N-labeled tracers and measured the subsequent $\delta^{15}N$ values of N_2O. This method is more sensitive than quantifying differences in N_2O concentration over time and has previously been used to obtain nitrification rate estimates (*e.g.* Barnes and Owens, 1999; Punshon and Moore, 2004). Upon recovery of the sediment traps, the collected material from each trap was filtered through a 335 μm Nitex screen and then siphoned into gas-tight 240 mL borosilicate glass vials and amended with either ^{15}N labeled NH_4Cl ($^{15}NH_4$), ^{15}N labeled $NaNO_2$ ($^{15}NO_2$), or ^{15}N labeled $NaNO_3$ ($^{15}NO_3$) (final concentration of all amendments was 4 μmol L^{-1}) (Table 1). The samples were incubated at 25 °C using a 12 h light:dark cycle, with a light level of 20 μmol photons m^{-2} s^{-1} which is approximately equivalent to the 0.1% light level found at the base of the euphotic zone. After 48 h, the incubation was terminated and the samples preserved with the addition of $HgCl_2$. The ^{15}N-labeled seawater samples were then analyzed for $\delta^{15}N$ values of N_2O, as described in Section 2.2.

During the February 2013 cruise, seawater was also collected from the same depth (150 m) as the sediment trap array using the CTD-rosette and similarly amended with $^{15}NH_4^+$ or $^{15}NO_2^-$ to obtain a final concentration of 4 μmol L^{-1}. The purpose of these water column measurements was to investigate N_2O production in free-living microorganisms and those attached to suspended particles, to complement the results previously obtained for

sediment trap-collected sinking particles. A final experiment was conducted during HOT cruise 253 (June 2013) to examine possible interactions between nitrification and nitrifier-denitrification pathways. Seawater was similarly collected from 150 m and amended with varying concentrations of NH_4^+ and NO_2^-. The seawater incubations contained either ^{15}N-labeled or unlabeled NH_4^+ and NO_2^-, and the four treatments consisted of (a) 0.1 μM $^{15}NH_4^+$ plus 1 μM NO_2^-, (b) 1 μM $^{15}NH_4^+$ plus 1 μM NO_2^-, (c) 0.1 μM NH_4^+ plus 1 μM $^{15}NO_2^-$, and (d) 1 μM NH_4^+ plus 1 μM $^{15}NO_2^-$. Therefore the concentration of NO_2^- was either equal to the concentration of NH_4^+ or exceeded it 10-fold. After incubating for 48 h, the samples were analyzed for the $\delta^{15}N$ values of N_2O as described above.

3. Results

3.1. Water column biogeochemistry

During the September 2011 cruise, the mixed layer depth varied from 20 to 70 m and seawater temperature in the mixed layer ranged from 25.1 to 26.4 °C. In comparison at 150 m depth, near the base of the euphotic zone, the seawater temperature averaged 20.9 °C. In February 2013, the mixed layer was deeper, averaging 131 m, and the average seawater temperature was 23 °C. Because the objective of this study was to evaluate the potential for N_2O production via NO_2^- metabolism in the surface ocean, an overview of the biogeochemistry in the upper water column is provided from the perspective of the N cycle. The upper-ocean N inventories measured during the September 2011 oceanographic cruise have also been compared with the HOT program measurements at Stn ALOHA from the previous 23 years to provide further contextual information (Table 2).

As characteristic of the oligotrophic ocean, both NO_2^- and NO_3^- concentrations were low (< 0.01 μmol L^{-1}) in the upper 50 m of the water column (Table 2). NO_3^- concentrations exceeded 1 μmol L^{-1} below 160 m as the persistent deep nutricline was encountered (Fig. 2). In contrast to the increasing concentrations of NO_3^- at the base of the euphotic zone, the presence of NO_2^- was limited to the PNM which was consistently located 20 m beneath the Deep Chlorophyll Maximum (DCM) (Fig. 2). Maximum NO_2^- concentrations at the PNM measured during a total of 11 vertical profiles extended up to 195 nmol L^{-1}. While the absolute depth of the PNM varied from 125 to 150 m, it consistently tracked the 24.6 kg m^{-3} isopycnal for a

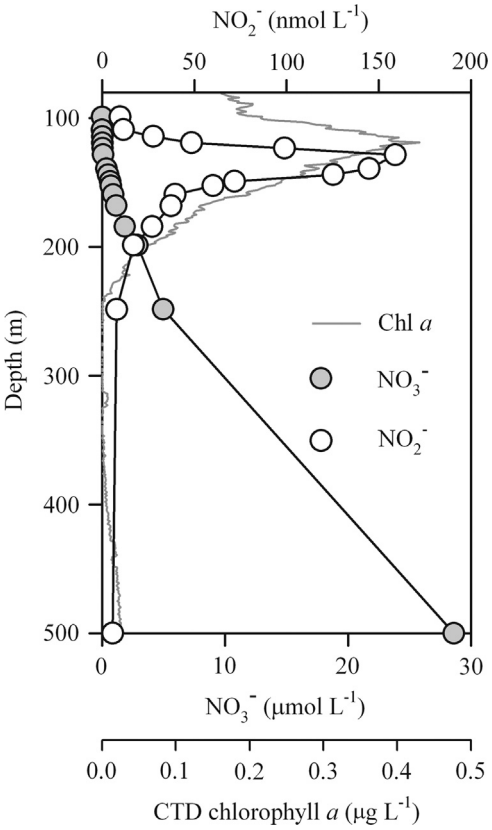

Fig. 2. Vertical profiles of NO_2^-, NO_3^-, and CTD chl *a*+phaeopigments measured between 100 and 500 m. Seawater samples were collected on September 10, 2011 at 24° 51.57N, 157° 28.01W.

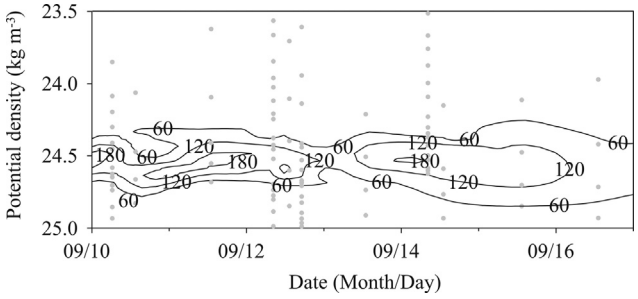

Fig. 3. NO_2^- concentrations near the base of the euphotic zone in September 2011. The NO_2^- maximum tracked the isopycnal corresponding to a potential density of 24.5 kg m^{-3} throughout the 7-day period shown.

Table 2
Inventories of selected N pools during the cruise in comparison to the HOT program at Stn ALOHA. The values for each parameter are compared for the surface seawater (0–50 m) and the base of the euphotic zone (125–175 m). Only the upper value is reported when the concentrations extend below detection level. NO_{2+3} (0–50 m) values are reported from the chemiluminescent method and NO_{2+3} (125–175 m) were measured using the autoanalyzer. NO_2^- were collected from 1989 to 1994 and N_2O were collected from 1994 to 1998.

Parameter	Depth horizon (m)	This study Sept 2011 (24° 40′N, 158°W)	HOT 1988–2011 (22°45′N, 158°W)
NO_2^-	0–50	≤ 7 nmol L^{-1}	≤ 4.7 nmol L^{-1}
	125–175	14–207 nmol L^{-1}	≤ 244 nmol L^{-1}
NO_{2+3}	0–50	≤ 0.006 μmol L^{-1}	≤ 0.06 μmol L^{-1}
	125–175	0.1–2.3 μmol L^{-1}	≤ 5.4 μmol L^{-1}
N_2O	0–50	–	6–9 nmol L^{-1}
	125–175	8.3–10.2 nmol L^{-1}	6–14 nmol L^{-1}
DON	0–50	–	3.5–9.2 μmol L^{-1}
	125–175	–	2.7–8.9 μmol L^{-1}
PON	0–50	0.3–0.5 μmol L^{-1}	0.2–0.8 μmol L^{-1}
	125–175	0.1–0.3 μmol L^{-1}	0.02–0.6 μmol L^{-1}

period of 7 days (Fig. 3). The PNM was always slightly asymmetrical in shape, revealing a tailing in NO_2^- concentrations with increasing depth (Fig. 2).

In contrast to the depth distribution of inorganic nutrients, concentrations of PON are maximal in near-surface waters, ranging from 0.3 to 0.5 μmol L^{-1} during September 2011. PON concentrations decreased with increasing depth and are 2–3 times lower at 150 m, where concentrations ranged from 0.1 to 0.3 μmol L^{-1}. Although not measured during this study, concentrations of dissolved organic N (DON) are typically 4–6 μmol L^{-1} in the upper 200 m of the water column (Table 2) (Karl et al., 2008).

Vertical profiles of N_2O were conducted during the study. Shown in Fig. 4A is a depth profile of dissolved N_2O and O_2 concentrations in the lower euphotic zone between 100 and 300 m. The N_2O profile was conducted at the same time as the NO_2^- profile shown in Fig. 2. Concentrations increased with depth from 7.9 nmol L^{-1} at 100 m to 12.1 nmol L^{-1} at 300 m and were consistently supersaturated with

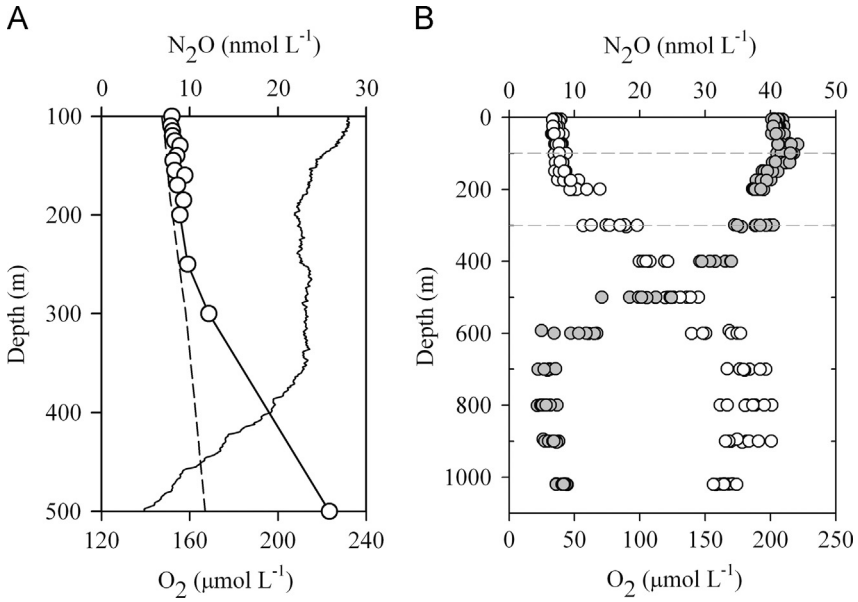

Fig. 4. (A) Vertical profiles of N_2O (open symbols) and O_2 (solid line) between 100 and 300 m sampled on September 10, 2011. The dashed line represents theoretical concentrations of N_2O in equilibrium with the atmosphere. (B) Vertical profiles of N_2O (open symbols) and O_2 (grey symbols) between 5 and 1000 m measured at Stn ALOHA during 2012. The horizontal grey lines show the depth range of the profile conducted on September 10, 2011.

respect to atmospheric equilibrium. To place this relatively narrow depth horizon of N_2O measurements into a wider water column context, vertical profiles of N_2O and O_2 collected at Stn ALOHA throughout 2012 extending from the surface to a depth of 1000 m are also shown (Fig. 4B). The clear increase in N_2O concentrations with depth coincides with a decrease in O_2 concentrations which reach a minimum at Stn ALOHA at 780 m.

3.2. Sediment trap experiments

The free-drifting sediment traps proved successful to investigate remineralization of organic material in relation to N cycling in the upper water column. In the preserved traps deployed with formalin, the sinking PON flux at a depth of 100 m was 550 μmol N m^{-2} d^{-1} and by 150 m this flux had decreased to 390 μmol N m^{-2} d^{-1} indicating efficient particle remineralization in the upper portion of the water column (Fig. 5a) The concentration of NH_4^+ measured in the preserved sediment trap solutions (and therefore reported as downward fluxes of particle-associated NH_4^+) revealed NH_4^+ production associated with sinking particulate material consistent with particle remineralization. The flux of particle- associated NH_4^+ measured in traps situated between 100 and 130 m ranged from 44 to 95 μmol m^{-2} d^{-1} and decreased with increasing depth to 0-8 μmol m^{-2} d^{-1} at the traps located between 200 and 500 m (Fig. 5b). In comparison, the downward flux of particle-associated NO_2^- ranged from 1.7 to 2.4 μmol m^{-2} d^{-1} with no observed variation with depth; NO_3^- was only detected at 500 m where the flux was 16 μmol m^{-2} d^{-1} (Fig. 5c).

A greater insight into the dynamics of N_2O associated with sinking particulate material was obtained with the nutrient-amended (NH_4^+ or NO_2^-) traps. Concentrations of dissolved N_2O resulting from these experimental manipulations are reported as N_2O accumulations (nmol L^{-1}) for ease of comparison with the water-column profiles (Fig. 4). N_2O accumulations can be converted to flux of particle-associated N_2O, as per the values in Fig. 6, using the cross-sectional area of the sediment trap (0.0039 m^2) and the deployment period (8 days). No significant accumulation of N_2O was recorded in the unamended trap (Fig. 6A). Accumulation of N_2O in the NH_4^+ amended trap ranged from 4.9 to 6.9 nmol L^{-1} with the maximum values measured in the trap situated at a depth of 150 m (Fig. 6B). The increases in N_2O accumulation as a result of NH_4^+ addition were significant (Student's *t*-test, $p=0.006$) when comparing all twelve NH_4^+ amended traps with the unamended trap samples. In response to the NO_2^- amendments, N_2O accumulations showed a significant increase (Student's *t*-test, $p=0.01$) (Fig. 6C). The accumulation of dissolved N_2O for traps amended with NO_2^- ranged from 5.1 to 13.7 nmol L^{-1}, representing over a 2-fold increase from the unamended traps (Fig. 6A). As observed for the NH_4^+ amended traps, the accumulation of N_2O was seemingly limited to the euphotic zone with no accumulation of N_2O observed in traps situated between 200 and 500 m. The O_2 concentrations for each trap is shown in Fig. 6D, also reported as O_2 concentrations (μmol L^{-1}) for comparison with the water-column profiles (Fig. 4). O_2 consumption was most pronounced in the traps situated between 100 and 150 m where final concentrations ranged from 174 to 188 μmol L^{-1}. No differences were observed in O_2 consumption rates in response to the addition of either NH_4^+ or NO_2^- (Fig. 6D). The final PON concentration for all three treatments (unamended, NH_4^+ amended, and NO_2^- amended) is shown in Fig. 6E and no significant difference was observed between the PON fluxes in response to the nutrient addition.

3.3. ^{15}N-amendment experiments

The unexpected increase in N_2O production with the addition of NO_2^- prompted subsequent experiments in February 2013 to corroborate this finding. This second set of experiments measured the changes $\delta^{15}N$ values of N_2O in samples collected from both sediment traps deployed at 150 m and the ambient water column at 150 m depth and amended with different ^{15}N compounds (Table 3). In the sediment trap samples, there was no significant difference in $\delta^{15}N$–N_2O values (Student's *t*-test, $P>0.05$) when $^{15}NH_4^+$ and $^{15}NO_3^-$ were added to the samples (5.6 ± 1.0 and 5.4 ± 0.3, respectively) relative to the control treatment (4.9 ± 1.0). In contrast, the addition of $^{15}NO_2^-$ stimulated a significant increase in $\delta^{15}N$–N_2O values (157.4 ± 22.6) (Student's *t*-test, $p=0.004$, $P<0.01$) in the sediment trap samples (Table 3). In comparison, for the water column samples, the $\delta^{15}N$–N_2O value was higher with the addition of $^{15}NO_2^-$ (16.6 ± 1.7) (Student's *t*-test, $p=0.03$, $P<0.05$) compared

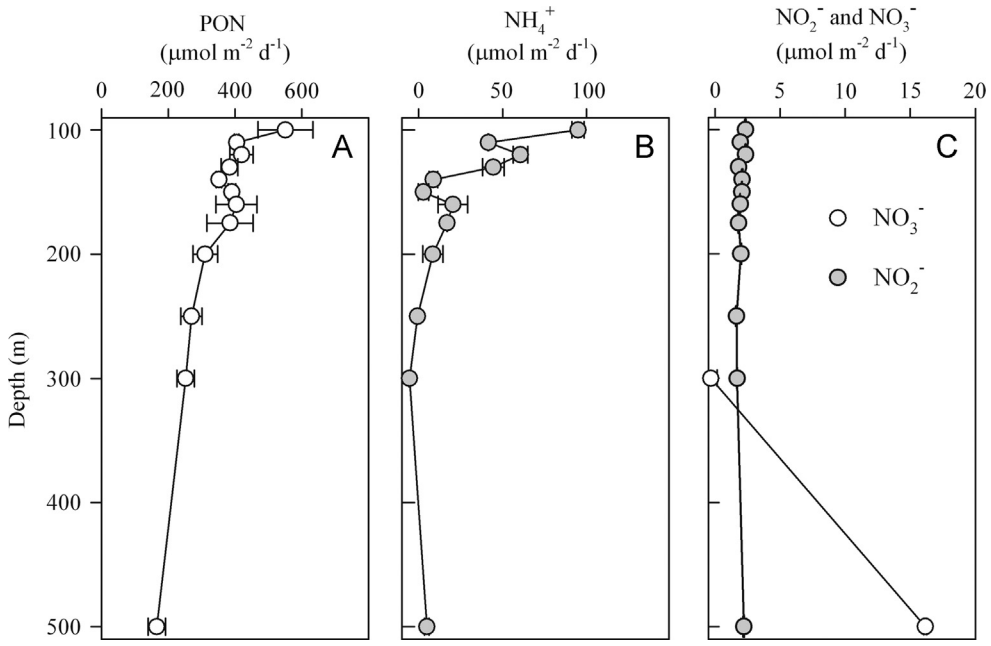

Fig. 5. Remineralization of nitrogen species associated with sinking particles collected at 12 discrete depths between 100 and 500 m in the water column during an 8 day deployment of free drifting sediment trap array in September 2011. Measurements included (A) PON, (B) NH_4^+, (C) NO_2^- and NO_3^-.

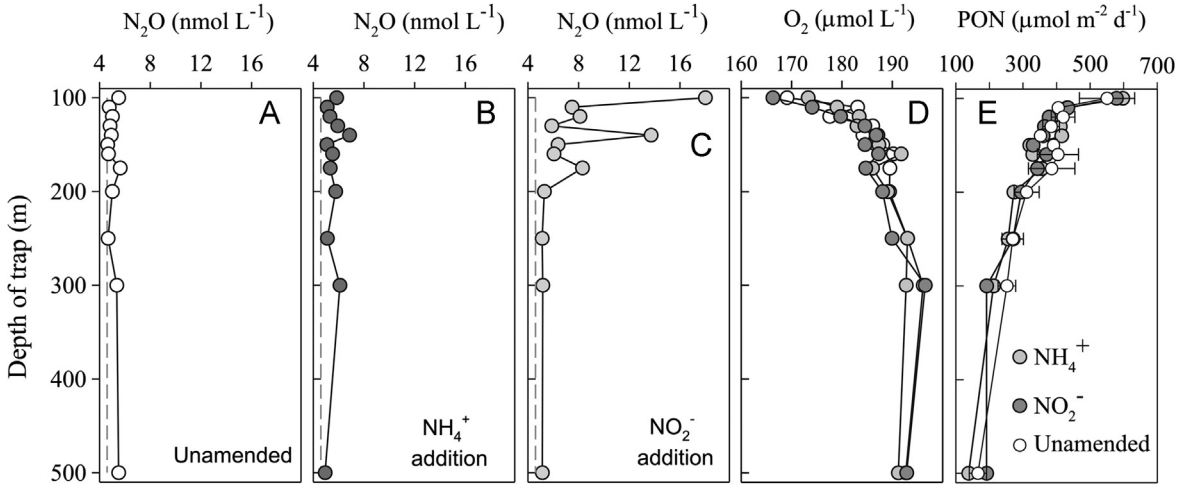

Fig. 6. N_2O accumulation associated with sedimenting particles situated between 100 and 500 m in the water column. N_2O concentrations were measured in (A) unamended, (B) NH_4^+ amended, and (C) NO_2^- amended sediment traps. The dashed lines represent the initial N_2O concentration prior to deployment of the array. The O_2 concentrations and PON fluxes in the three experimental sediment traps are shown in (D) and (E), respectively. The traps were deployed from September 9–17, 2011.

to the addition of $^{15}NH_4^+$ (5.6 ± 2.6) (Student's *t*-test, $p = 0.02$, $P < 0.05$). In the unamended samples from the water column, the $\delta^{15}N$–N_2O value was 3.4 ± 1.8 and no addition of $^{15}NO_3^-$ was made to seawater collected from 150 m.

The second set of water-column experiments in June 2013 measured the changes in $\delta^{15}N$ values of N_2O when the concentrations of NH_4^+ were varied to be either less than or equivalent to the concentration of NO_2^-. The highest $\delta^{15}N$ values of N_2O ($\delta^{15}N$–N_2O ranged from 19.3 to 20.0) occurred in the presence of $^{15}NO_2^-$ when NO_2^- concentrations (1 μM) exceeded NH_4^+ concentrations (0.1 μM) (Table 4). When the quantity of NH_4^+ added to the seawater samples was increased to equal the concentration of NO_2^-, the $\delta^{15}N$ values of N_2O were lower ($\delta^{15}N$–N_2O ranged from 5.5 to 5.8) compared to the $^{15}NO_2^-$-labeled samples. In comparison, in the presence of $^{15}NH_4^+$, $\delta^{15}N$ values of N_2O were lower ($\delta^{15}N$–N_2O ranged from 4.7 to 4.8), supporting the findings from the water column measurements conducted in February 2013 (Table 4).

4. Discussion

The lower euphotic zone represents a possible habitat for the selection of nitrifier-denitrification microbial metabolism in the oligotrophic open ocean. The low ambient light intensity and the elevated NO_2^- concentrations, which in this study ranged up to 0.2 μmol L^{-1}, increase the potential for ammonia-oxidizing microorganisms to be involved in NO_2^- metabolism. In culture-based studies, the common indicator for nitrifier-denitrifying activity is an increase in N_2O yield with the addition of NO_2^- (Goreau et al., 1980; Poth and Focht, 1985; Frame and Casciotti, 2010). However in the open ocean there is no conspicuous increase in dissolved N_2O concentrations associated with the PNM which would indicate a direct connection with the cycling of NO_2^- (Fig. 4A). Vertical profiles of N_2O concentrations in the water column show a continual increase with depth between 100 m and the O_2 minimum at 780 m (Fig. 4B). It cannot be ruled out that a small increase at the base of the euphotic zone is

Table 3
Changes in the nitrogen isotopic composition of N_2O following the addition of ^{15}N-labeled substrates to seawater collected in Niskin bottles and particles collected using sediment traps. All samples were collected in February 2013 and $\delta^{15}N$ values of N_2O are reported in permil relative to atmospheric N_2. The uncertainty in the $\delta^{15}N$ values of N_2O is represented by standard deviation for the samples amended with sediment trap materials ($n=3$) and propagated error for water column samples (duplicate samples analyzed from triplicate bottles). The statistical significance (Sig. level) of each treatment in comparison with the unamended sample was calculated using Student's *t*-test.

Treatment	Sediment trap		Water column	
	$\delta^{15}N$, ‰	Sig. level	$\delta^{15}N$, ‰	Sig. level
Unamended	4.9 ± 1.1	–	3.4 ± 1.8	–
$^{15}NH_4^+$-amended	5.6 ± 1.0	ns	5.6 ± 2.6	*
$^{15}NO_2^-$-amended	157.4 ± 22.6	**	16.6 ± 1.7	*
$^{15}NO_3^-$-amended	5.4 ± 0.3	ns	–	–

ns = Not significant = $P > 0.05$.
* $P < 0.05$.
** $P < 0.01$.

Table 4
Changes in the nitrogen isotopic composition of N_2O in seawater samples collected from 150 m in June 2013 and amended with either labeled ^{15}N ($^{15}NH_4^+$ or $^{15}NO_2^-$) or unlabeled N (NH_4^+ or NO_2^-). The values from duplicate experiments are reported for each experiment ($n=2$) and $\delta^{15}N$ values of N_2O are reported in permil relative to atmospheric N_2.

Treatment	$^{15}NH_4^+$-labeled $\delta^{15}N$, ‰	Treatment	$^{15}NO_2^-$-labeled $\delta^{15}N$, ‰
1 μM NO_2^- 0.1 μM $^{15}NH_4^+$	4.7–4.8	1 μM $^{15}NO_2^-$ 0.1 μM NH_4^+	19.3–20.0
1 μM NO_2^- 1 μM $^{15}NH_4^+$	4.8–5.0	1 μM $^{15}NO_2^-$ 1 μM NH_4^+	5.5–5.8

obscured by the larger signal of an increase in N_2O concentrations with depth.

Another apparently suitable habitat for ammonia-oxidizing microorganisms in the upper water column is sinking particles. Particles represent important habitats for microbial activity in the water column (Alldredge et al., 1986; Kiørboe and Jackson, 2001) which may be particularly relevant for chemolithotrophic microorganisms (Karl et al., 1984). Enhanced activity of ammonia-oxidizing microorganisms is considered particularly likely in the unamended sediment traps situated between 100 and 200 m where particle-associated NH_4^+ fluxes range from 2 to 4 μmol m^{-2} d^{-1} (Fig. 5B). However there was no measurable increase in either NO_2^- or N_2O in the unamended sediment traps. It has been suggested that nitrification predominantly occurs in the water column rather than rapidly sinking particles (which could occur from the oxidation of the NH_4^+ released from the decomposition of particles) (Ward, 2008). The absence of either NO_2^- or N_2O fluxes in the sediment trap profiles in this study appears to support this hypothesis.

It is clear that the hydrographic, biogeochemical, and particle-associated flux profiles described so far are insufficient to understand the pathways of N_2O production in the oligotrophic water column. Therefore we conducted a series of incubation experiments using water samples and collections of sinking particles to investigate potential mechanisms of N_2O production. The initial sediment trap array, deployed for an 8 day period in September 2011, included unpreserved traps that were amended with NO_2^- and NH_4^+ at concentrations exceeding the PON concentration in the sediment trap situated at 100 m by 4–6 fold. Subsequent follow-on experiments added lower concentrations of nutrients and the traps were deployed for a shorter period. The noteworthy finding in these experiments is that the highest accumulations of N_2O were observed with the amendment of NO_2^- rather than NH_4^+ (Fig. 6). The N_2O accumulations in trap samples were limited to those situated between 100 and 175 m which could reflect changes in particle constitution during export, the influence of an upper water-column hydrographic or biogeochemical component, or another unidentified factor. The increase in $\delta^{15}N$ values of N_2O with the addition of $^{15}NO_2^-$ to water column samples reveal that the process responsible is not limited to sinking particles (Tables 3 and 4). Based on our current understanding of the marine N cycle, we attribute the production of N_2O from NO_2^- to nitrifier-denitrification metabolism.

Supporting evidence that nitrifier-denitrification is occurring in the water column is provided by previous work analyzing the isotopic signatures of N_2O and O_2. Early isotopic studies at Stn ALOHA measured the ^{15}N and ^{18}O signatures of N_2O in the water column to reveal that nitrification was the most probable source of N_2O in the surface ocean (Dore et al., 1998). Of particular relevance to this current study is that when the isotopic measurements were expanded to include the $\delta^{18}O$ of H_2O and dissolved O_2, a distinct minimum in $\Delta^{18}O$ values (representing the difference between $\delta^{18}O$ of N_2O and O_2) was found between 200 and 500 m in the water column (Ostrom et al., 2000). These $\Delta^{18}O$ values taken alongside the $\delta^{15}N$ values at the same depths are indicative of a nitrifier-denitrifier mechanism producing N_2O. Furthermore, this minimum in $\Delta^{18}O$ values at 200–500 m has been observed in both the North Pacific (Popp et al., 2002) and South Pacific (Charpentier et al., 2007) Subtropical Gyre ecosystems. It is noted that the sediment traps associated with N_2O accumulations were situated between 100 and 200 m and therefore slightly shallower than the reported minimum in $\Delta^{18}O$ values (Ostrom et al., 2000). This may be explained, in part, by the fact that the sinking particles collected at 150 m would normally continue to sink at rates of tens to hundreds of meters per day contributing to the isotopic signature of gaseous metabolic by-products throughout the mesopelagic zone.

The existence of nitrifier-denitrification activity leads to questions regarding the microorganisms responsible and the environmental variables that control their activity. The genomic studies to date of nitrifying bacteria and nitrifying archaea (*Cenarchaeum symbiosum* and *Nitrosopumilus maritimus*) reveal the presence of the genes required for either full or partial denitrification (Arp et al., 2007; Hallam et al., 2006; Walker et al., 2010). Metatranscriptomic studies at Stn ALOHA found that expression ratios of nitrite reductases nearly equaled those of *amoA* (the gene encoding the active subunit of ammonia monooxygenase), highly expressed at 500 m (Shi et al., 2011). Furthermore, the *nirK* (and *amoA*) gene transcripts were detected in high abundance relative to gene abundance at a depth of 125 m, despite the Thaumarchaea population size at that depth being lower than in the mesopelagic ocean (Karner et al., 2001). A latitudinal transect across the Pacific Ocean similarly revealed elevated Thaumarchaeal *amoA* expression in the upper ocean waters (0–100 m) where Thaumarchaeal abundances were low, in comparison to the mesopelagic zone where high gene abundances coincided with low transcripts (Church et al., 2009). Therefore the molecular evidence also supports the potential for nitrifier-denitrification although it is not clear what 'activates' this metabolic pathway. To date, the majority of culture-based studies have focused on the yield of N_2O under changing O_2 concentrations (*e.g.* Goreau et al., 1980) and it has been interpreted that *Nitrosomonas* sp. may use NO_2^- as a terminal electron acceptor under conditions of O_2 stress (Poth and Focht, 1985). However it should be noted that more recent culture-based studies of *Nitrosomonas* sp. provide evidence that O_2 might not be the dominant influence on nitrifier-denitification activity (Beaumont et al., 2004; Frame and Casciotti, 2010). In the pelagic environment, sinking particles are often considered to support localized low O_2 concentrations due to the enhanced particle-associated microbial activity.

Another influence on nitrifier-denitrification is the relative availability of NO_2^- and NH_4^+ for ammonia-oxidizing microorganisms. Experiments investigating the relationship between nitrification and nitrifier-denitrification indicate that the latter pathway is stimulated when NO_2^- concentrations exceed the NH_4^+ concentrations (Table 4). This finding is not surprising, although to our knowledge the effect of NO_2^- and NH_4^+ availability on nitrifier-denitrification has not been investigated in either the open ocean or culture-based studies. The relative increase in $\delta^{15}N$–N_2O values when NO_2^- is in excess of dissolved NH_4^+ strengthen the significance of the PNM as a potential location in the water column for nitrifier-denitrification metabolism. Although water column measurements of NH_4^+ were not conducted in this study and there are limited high-resolution profiles of NH_4^+ in the open ocean, it is expected that NO_2^- concentrations exceed NH_4^+ concentrations at the peak of the PNM (Fig. 2). Vertical NH_4^+ profiles indicate an offset between the NO_2^- peak associated with the PNM and maximum NH_4^+ concentrations which can occur closer to the ocean surface (Woodward and Rees, 2001; Raimbault et al., 2008; Santoro et al., 2013).

Finally, we consider the ecological consequences of nitrifier-denitrification occurring in the upper water column. It has previously been shown that *in situ* production of N_2O in the euphotic zone at Stn ALOHA is responsible for supersaturating N_2O concentrations in the surface seawater (Dore and Karl, 1996a) and this study shows nitrifier-denitrification is a potential source of N_2O. Nitrifier-denitrification also represents an example of nitrogen-based microbial metabolism which does not drive N oxidation to NO_3^-. Measured NO_3^- concentrations between 100 and 200 m depth at Stn ALOHA are lower than predicted using a NO_3^-/AOU stoichiometry (Emerson and Hayward, 1995; Johnson et al., 2010). Nitrifier-denitrification activity is a potential contributing mechanism in addition to other pathways discussed in Emerson and Hayward (1995). These two examples highlight the repercussions of nitrifier-denitrification and indicate NO_2^- is a key redox intermediate in the euphotic zone and thereby plays an important role in the N cycle (Emerson and Hayward, 1995; Karl et al., 2008).

5. Conclusion

The potential for N_2O production via NO_2^- metabolism in the upper water column is an intriguing prospect for understanding the dynamics of N_2O cycling in the open ocean. This study revealed increased $\delta^{15}N$ values of N_2O when seawater and sinking particles are amended with $^{15}NO_2^-$, compared to the addition of $^{15}NH_4^+$. This finding supports nitrifier-denitrification as a potential source of N_2O in the lower euphotic zone. However the relationship between the nitrifier-denitrification pathway and the dissolved pools of NH_4^+, NO_2^-, DON, and N_2O in the upper water column is not well understood at present. Furthermore, there may well be other, currently unidentified, sources of N_2O. Resolving the environmental constraints on nitrifier-denitrification will help to understand N_2O dynamics in the open ocean and indicate how future changes in physical and biogeochemical characteristics of the water column influence the source of this important greenhouse gas.

Acknowledgements

We are grateful to the chief scientists Julie Robidart for the September 8–22 cruise in 2011 and Susan Curless for HOT 249 and HOT 253 in 2013, respectively. We also thank Tara Clemente, Eric Grabowski, Ariel Rabines, Ben Rubin, and Blake Watkins who assisted with sample collection and analysis. Brian Popp and the Stable Isotope Facility at the University of Hawaii provided technical and essential advice for the tracer studies. We thank the R/V *Kilo Moana* captain and crew for their continuing support of oceanographic research. Three anonymous reviewers provided critical and useful comments that improved the manuscript. This research was supported by the National Science Foundation Center for Microbial Oceanography: Research and Education (C-MORE) (EF0424599 to D.M.K., P.I.), NSF Grant OCE-1153656 (D.M.K., P.I.) and the Gordon and Betty Moore Foundation Marine Microbiology Investigator awards to D.M.K.

References

Alldredge, A.L., Cole, J.J., Caron, D.A., 1986. Production of heterotrophic bacteria inhabiting macroscopic organic aggregates (marine snow) from surface waters. Limnol. Oceanogr. 31 (1), 68–78.

Arp, D.J., Chain, P.S.G., Klotz, M.G., 2007. The impact of genome analyses on our understanding of ammonia-oxidizing bacteria. Annu. Rev. Microbiol. 61, 503–528.

Bange, H.W., Freing, A., Kock, A., Löscher, C.R., 2010. Marine pathways to nitrous oxide. In: Smith, K.A. (Ed.), Nitrous Oxide and Climate Change. Earthscan, London, Washington, pp. 36–62.

Barnes, J., Owens, N.J.P., 1999. Denitrification and nitrous oxide concentrations in the Humber estuary, UK, and adjacent coastal zones. Mar. Pollut. Bull. 37 (3–7), 247–260.

Beaumont, H.J.E., Lens, S.I., Reijnders, W.N.M., Westerhoff, H.V., van Spanning, R.J. M., 2004. Expression of nitrite reductase in *Nitrosomonas europaea* involves NsrR, a novel nitrite-sensitive transcription repressor. Mol. Microbiol 54 (1), 148–158.

Carritt, D.E., Carpenter, J.H., 1966. Comparison and evaluation of currently employed modifications of the Winkler method for determining dissolved oxygen in seawater; a NASCO report. J. Mar. Res. 24, 286–318.

Charpentier, J., Farías, L., Yoshida, N., Boontanon, N., Raimbault, P., 2007. Nitrous oxide distribution and its origin in the central and eastern South Pacific Subtropical Gyre. Biogeosciences 4, 729–741.

Church, M.J., Wai, B., Karl, D.M., DeLong, E.F., 2009. Abundances of crenarchaeal *amoA* genes and transcripts in the Pacific Ocean. Environ. Microbiol. 12 (3), 679–688.

Denman, K.L., Brasseur, G., Chidthaisong, A., Ciais, P., Cox, P.M., Dickinson, R.E., Hauglustaine, D., Heinze, C., Holland, E., Jacob, D., Lohmann, U., Ramachandran, S., da Silva Dias, P.L., Wofsy, S.C., Zhang, X., 2007. Couplings between changes in the climate system and biogeochemistry. In: Solomon, S., Qin, D., Manning, M., Chen, Z., Marquis, M., Averyt, K.B., Tignor, M., Miller, H.L. (Eds.), Climate Change 2007: The Physical Science Basis. Contribution of Working Group I to the Fourth Assessment Report of the Intergovernmental Panel on Climate Change. Cambridge University Press, Cambridge, UK, New York, NY.

Dore, J.E., Karl, D.M., 1996a. Nitrification in the euphotic zone as a source for nitrite, nitrate, and nitrous oxide at Station ALOHA. Limnol. Oceanogr. 41 (8), 1619–1628.

Dore, J.E., Karl, D.M., 1996b. Nitrite distributions and dynamics at Station ALOHA. Deep Sea Res. Part II 43 (2–3), 385–402.

Dore, J.E., Popp, B.N., Karl, D.M., Sansone, F.J., 1998. A large source of atmospheric nitrous oxide from subtropical North Pacific surface waters. Nature 396 (6706), 63–66.

Emerson, S., Hayward, T.L., 1995. Chemical tracers of biological processes in shallow waters of the North Pacific: preformed nitrate distributions. J. Mar. Res. 53 (3), 499–513.

Forster, G., Upstill-Goddard, R.C., Gist, N., Robinson, C., Uher, G., Woodward, E.M.S., 2009. Nitrous oxide and methane in the Atlantic Ocean between 50°N and 52°S: latitudinal distribution and sea-to-air flux. Deep Sea Res. Part II 56 (15), 964–976.

Frame, C.H., Casciotti, K.L., 2010. Biogeochemical controls and isotopic signatures of nitrous oxide production by a marine ammonia-oxidizing bacterium. Biogeosciences 7, 2695–2709.

Francis, C.A., Roberts, K.J., Beman, J.M., Santoro, A.E., Oakley, B.B., 2005. Ubiquity and diversity of ammonia-oxidizing archaea in water columns and sediments of the ocean. Proc. Nat. Acad. Sci 102 (41), 14683–14688.

Goreau, T.J., Kaplan, W.A., Wofsy, S.C., McElroy, M.B., Valois, F.W., Watson, S.W., 1980. Production of NO_2^- and N_2O by nitrifying bacteria at reduced concentrations of oxygen. Appl. Environ. Microbiol 40 (3), 526–532.

Hallam, S.J., Mincer, T.J., Schleper, C., Preston, C.M., Roberts, K., Richardson, P.M., DeLong, E.F., 2006. Pathways of carbon assimilation and ammonia oxidation suggested by environmental genomic analyses of marine *Crenarchaeota*. PLoS Biol. 520–536, e95.

Hansen, H.P., Koroleff, F., 1999. Determination of nutrients. In: Grasshoff, K., Kremling, K., Ehrhardt, M. (Eds.), Methods of Seawater Analysis, third ed. Wiley, New York, pp. 75–89.

Johnson, K.S., Riser, S.C., Karl, D.M., 2010. Nitrate supply from deep to near-surface waters of the North Pacific Subtropical Gyre. Nature 465 (7301), 1062–1065.

Kana, T.M., Darkangelo, C., Duane Hunt, M., Oldham, J.B., Bennett, G.E., Cornwell, J.C., 1994. Membrane inlet mass spectrometer for rapid high-precision determination of N_2, O_2, and Ar in environmental water samples. Anal. Chem. 66 (23), 4166–4170.

Karl, D.M., Knauer, G.A., 1989. Swimmers: a recapitulation of the problem and a potential solution. Oceanogr. Mag. 2, 32–35.
Karl, D.M., Knauer, G.A., Martin, J.H., Ward, B.B., 1984. Bacterial chemolithotrophy in the ocean is associated with sinking particles. Nature 309 (5963), 54–56.
Karl, D.M., Lukas, R., 1996. The Hawaii Ocean Time-series (HOT) program: background, rationale and field implementation. Deep Sea Res. Part II 43 (2–3), 129–156.
Karl, D.M., Bidigare, R.R., Church, M.J., Dore, J.E., Letelier, R.M., Mahaffey, C., Zehr, J.P., 2008. The nitrogen cycle in the North Pacific trades Biomes: an evolving paradigm. In: Capone, D.G., Bronk, D.A., Mulholland, M.R., Carpenter, E.J. (Eds.), Nitrogen in the Marine Environment, second ed. Elsevier, Amsterdam, pp. 705–769.
Karner, M.B., DeLong, E.F., Karl, D.M., 2001. Archaeal dominance in the mesopelagic zone of the Pacific Ocean. Nature 409 (6819), 507–510.
Kiefer, D., Olson, R., Holm-Hansen, O., 1976. Another look at the nitrite and chlorophyll maxima in the central North Pacific. Deep Sea Res 23 (12), 1199–1208.
Kiørboe, T., Jackson, G.A., 2001. Marine snow, organic solute plumes, and optimal chemosensory behavior of bacteria. Limnol. Oceanogr. 46 (6), 1309–1318.
Knauer, G.A., Martin, J.H., Bruland, K.W., 1979. Fluxes of particulate carbon, nitrogen and phosphorus in the upper water column of the northeast Pacific. Deep Sea Res 26 (1), 97–108.
Lomas, M.W., Lipschultz, F., 2006. Forming the primary nitrite maximum: nitrifiers or phytoplankton? Limnol. Oceanogr 51 (5), 2453–2467.
Löscher, C.R., Kock, A., Könneke, M., LaRoche, J., Bange, H.W., Schmitz, R.A., 2012. Production of oceanic nitrous oxide by ammonia-oxidizing archaea. Biogeosciences 9 (7), 2419–2429.
Mincer, T.J., Church, M.J., Taylor, L.T., Preston, C., Karl, D.M., DeLong, E.F., 2007. Quantitative distribution of presumptive archaeal and bacterial nitrifiers in Monterey Bay and the North Pacific Subtropical Gyre. Environ. Microbiol. 9 (5), 1162–1175.
Nevison, C.D., Butler, J.H., Elkins, J.W., 2003. Global distribution of N_2O and the ΔN_2O-AOU yield in the subsurface ocean. Global Biogeochem. Cycles 17 (10). (1029/2003GB002068).
Olson, R.J., 1981. Differential photoinhibition of marine nitrifying bacteria: a possible mechanism for the formation of the primary nitrite maximum. J. Mar. Res. 39, 227–238.
Ostrom, N.E., Russ, M.E., Popp, B., Rust, T.M., Karl, D.M., 2000. Mechanisms of nitrous oxide production in the subtropical North Pacific based on determinations of the isotopic abundances of nitrous oxide and di-oxygen. Chemosphere —Global Change Sci. 2 (3–4), 281–290.
Popp, B.N., Sansone, F.J., Rust, T.M., Merritt, D.A., 1995. Determination of concentration and carbon isotopic composition of dissolved methane in sediments and nearshore waters. Anal. Chem. 67 (2), 405–411.
Popp, B.N., Westley, M.B., Toyoda, S., Miwa, T., Dore, J.E., Yoshida, N., Rust, T.M., Sansone, F.J., Russ, M.E., Ostrom, N.E., Ostrom, P.H., 2002. Nitrogen and oxygen isotopomeric constraints on the origins and sea-to-air flux of N_2O in the oligotrophic subtropical North Pacific Gyre. Global Biogeochem. Cycles 16 (4), 1064.
Poth, M., Focht, D.D., 1985. ^{15}N kinetic analysis of N_2O production by *Nitrosomonas europaea*: an examination of nitrifier denitrification. Appl. Environ. Microbiol 49 (5), 1134–1141.
Punshon, S., Moore, R.M., 2004. A stable isotope technique for measuring production and consumption rates of nitrous oxide in coastal waters. Mar. Chem. 86 (3–4), 159–168.
Raimbault, P., Garcia, N., Cerutti, F., 2008. Distribution of inorganic and organic nutrients in the South Pacific Ocean—evidence for long-term accumulation of organic matter in nitrogen-depleted waters. Biogeosciences 5 (2), 281–298.
Ravishankara, A.R., Daniel, J.S., Portmann, R.W., 2009. Nitrous oxide (N_2O): the dominant ozone-depleting substance emitted in the 21st century. Science 326 (5949), 123–125.
Rotthauwe, J.H., Witzel, K.P., Liesack, W., 1997. The ammonia monooxygenase structural gene *amoA* as a functional marker: molecular fine-scale analysis of natural ammonia-oxidizing populations. Appl. Environ. Microbiol 63 (12), 4704–4712.
Santoro, A.E., Casciotti, K.L., Francis, C.A., 2010. Activity, abundance and diversity of nitrifying archaea in the central California current. Environ. Microbiol. 12 (7), 1989–2006.
Santoro, A.E., Buchwald, C., McIlvin, M.R., Casciotti, K.L., 2011. Isotopic signature of N_2O produced by marine ammonia-oxidizing Archaea. Science 333 (6047), 1282–1285.
Santoro, A.E., Sakamoto, C.M., Smith, J.M., Plant, J.N., Gehman, A.L., Worden, A.Z., Johnson, K.S., Francis, C.A., Casciotti, K.L., 2013. Measurements of nitrite production and nitrite-producing organisms in and around the primary nitrite maximum in the central California current. Biogeosci. Discuss. 10, 5803–5840.
Shaw, L.J., Nicol, G.W., Smith, Z., Fear, J., Prosser, J.I., Baggs, E.M., 2006. *Nitrosospira* spp. can produce nitrous oxide via a nitrifier denitrification pathway. Environ. Microbiol. 8 (2), 214–222.
Shi, Y., Tyson, G.W., Eppley, J.M., DeLong, E.F., 2011. Integrated metatranscriptomic and metagenomic analyses of stratified microbial assemblages in the open ocean. ISME J 5 (6), 999–1013.
Strickland, J.D.H., Parsons, T.R., 1972. A Practical Handbook of Seawater Analysis. Fisheries Research Board of Canada, Ottawa, Ontario.
Sutka, R.L., Ostrom, N.E., Ostrom, P.H., Breznak, J.A., Gandhi, H., Pitt, A.J., Li, F., 2006. Distinguishing nitrous oxide production from nitrification and denitrification on the basis of isotopomer abundances. Appl. Environ. Microbiol 72 (1), 638–644.
Walker, C.B., de la Torre, J.R., Klotz, M.G., Urakawa, H., Pinela, N., Arp, D.J., Brochier-Armanet, C., Chain, P.S.G., Chan, P.P., Gollabgir, A., Hemp, J., Hügler, M., Karr, E.A., Könneke, M., Shin, M., Lawton, T.J., Lowe, T., Martens-Habbena, W., Sayavedra-Soto, L.A., Lang, D., Sievert, S.M., Rosenzweig, A.C., Manning, G., Stahl, D.A., 2010. *Nitrosopumilus maritimus* genome reveals unique mechanisms for nitrification and autotrophy in globally distributed marine crenarchaea. Proc. Nat. Acad. Sci 107 (19), 8818–8823.
Ward, B.B., 2008. Nitrification in marine systems. In: Capone, D.G., Bronk, D.A., Mulholland, M.R., Carpenter, E.J. (Eds.), Nitrogen in the Marine Environment, second ed. Elsevier, Amsterdam, pp. 199–261.
Weiss, R.F., Price, B.A., 1980. Nitrous oxide solubility in water and seawater. Mar. Chem. 8 (4), 347–359.
Woodward, E.M.S., Rees, A.P., 2001. Nutrient distributions in an anticyclonic eddy in the northeast Atlantic Ocean, with reference to nanomolar ammonium concentrations. Deep Sea Res 48 (4–5), 775–793.
Wrage, N., Velthof, G.L., van Beusichem, M.L., Oenema, O., 2001. Role of nitrifer denitrification in the production of nitrous oxide. Soil Biol. Biochem. 33, 1723–1732.